r-Process Nucleosynthesis in Hot Accretion Disk Flows from Black Hole - Neutron Star Mergers

R. Surman[1] and G. C. McLaughlin

Department of Physics, North Carolina State University, Raleigh, NC 27695-8202

M. Ruffert

School of Mathematics, University of Edinburgh, Edinburgh EH9 3JZ

H.-Th. Janka

Max-Planck-Institut für Astrophysik, Postfach 1317, 85741 Garching, Germany

and

W. R. Hix

Physics Division, Oak Ridge National Laboratory, Oak Ridge, TN 37831-6374

ABSTRACT

We consider hot accretion disk outflows from black hole - neutron star mergers in the context of the nucleosynthesis they produce. We begin with a three dimensional numerical model of a black hole - neutron star merger and calculate the neutrino and antineutrino fluxes emitted from the resulting accretion disk. We then follow the element synthesis in material outflowing the disk along parameterized trajectories. We find that at least a weak r-process is produced, and in some cases a main r-process as well. The neutron-rich conditions required for this production of r-process nuclei stem directly from the interactions of the neutrinos emitted by the disk with the free neutrons and protons in the outflow.

Subject headings: nuclear reactions, nucleosynthesis, abundances — neutrinos — stars: neutron

[1]Permanent Address: Department of Physics and Astronomy, Union College, Schenectady, NY 12308

1. Introduction

Compact object mergers, such as neutron star - neutron star (NS-NS) mergers or black hole - neutron star (BH-NS) mergers, have long been speculated to be a site of the r-process of nucleosynthesis (Lattimer & Schramm 1974, 1976). There are a number of different processes which can create ejecta during a merger. For both NS-NS and BH-NS mergers, cold, low entropy neutron star matter originating from the inner crust of the merging neutron star(s) can be ejected from tidal tails which form during the merger. Traditional calculations of nucleosynthesis from mergers have focused on this mechanism by calculating either cold decompression of neutron star matter, e.g. (Meyer 1989; Goriely et al. 2005) or mild heating of the matter to $T \sim 1$ MeV which leads to an (n, γ)-(γ, n) equilibrium, e.g. (Freiburghaus et al. 1999). Recently, Oechslin et al. (2007) have shown that in addition to the ejection from tidal tails, in the case of NS-NS mergers there is a second, hotter ($T \sim 10$ MeV) component that comes from the contact surface of the two merging neutron stars and is ejected perpendicular to the plane of the merger. As either a NS-NS or BH-NS merger progresses, an accretion torus surrounding a black hole is formed. Additional material can be ejected from the inner, hot region of the torus and/or the colder outer region, either out of the plane of the disk or escaping from the edges of the torus. Little calculation has been performed to date on the latter scenarios; we will focus here on ejecta from the inner hot region of the torus.

Understanding of the r-process of nucleosynthesis has undergone a dramatic transition in the last decade. Prior to this transition, it was a commonly held view that there was one primary process that contributed to the entire range of r-process nuclei; recent data from meteorites and metal-poor halo stars has changed that view (see Qian & Wasserburg (2007) and references therein). This data independently suggests that there is a main r-process which contributes to the heavier r-process elements above the second peak and a weak r-process that contributes to those below. Using timescale arguments based on the data further suggests that compact object mergers are not primarily responsible for the main r-process component seen in the metal poor halo stars (Argast et al. 2004), though a contribution may be possible if a second production mechanism for compact binaries exists that results in the creation of tighter orbits with faster decay timescales, as has been suggested by Belczynski et al. (2006). In any event compact binary mergers could possibly be a significant contributor to the weak r-process component as observed in the solar system today.

Interest in BH-NS mergers has recently intensified with the suggested correlation with short duration gamma ray bursts, e.g., Ruffert et al. (1997); Janka et al. (1999); Nakar (2007) and references therein. State of the art numerical models now include high-resolution shock-capturing hydrodynamics (on nested grids or with sufficiently high particle numbers) including some amount of relativistic effects and the ability to trace the nuclear composition, a matching microphysical equation-of-state, and including neutrino emission and its main effects on the emitting matter. This creates an excellent launching point for studies of nucleosynthesis.

In this letter we present the results of nucleosynthesis calculations for material in winds which leave the surface of the hot accretion disk formed by the merger of a black hole and a neutron star. We take special care with the neutrino fluxes, since neutrino interactions primarily set the electron fraction ($Y_e = \frac{p}{n+p}$), and therefore determine the outcome of the nucleosynthesis.

2. Black Hole - Neutron Star Merger Model

We simulate the merger of a non-rotating cool $1.6M_\odot$ neutron star and a $2.5M_\odot$ black hole with spin parameter 0.6. The hydrodynamics is evolved with the Piecewise Parabolic Method on grids with 128^3 zones nested 4 deep (Ruffert et al. 1996). Gravitational wave emission and neutrino emission is included as described in Ruffert & Janka (2001, and references therein). The black hole is treated as gravitating vacuum sphere with a modified potential (Artemova et al. 1996). The gas is described by equation of state of Shen et al. (1998). The simulation was evolved until the remains of the shredded neutron star formed a disk around the black hole, i.e. approximately 20 ms after initial contact.

From this model we have calculated neutrino surfaces, i.e. the places where the neutrinos decouple from the disk, using the method described in Surman & McLaughlin (2004). The results can be seen in Fig. 1 where we show the local disk temperatures at the point of decoupling, which we take to be the temperatures of thermal neutrino fluxes emitted from the disk. One can see that the spatial region of neutrino trapping exceeds that of antineutrino trapping but that the temperatures of the emitted $\bar{\nu}_e$ are greater than that of the emitted ν_e. As we will show, this has important consequences for the nucleosynthesis. We also show a vertical slice of the disk in Fig. 2.

3. Nucleosynthesis Calculation

Starting from this model of the disk, we proceed to calculate nucleosynthesis products in material outflowing the disk. We construct parameterized trajectories using the method outlined in Surman & McLaughlin (2005). We take the outflow to be adiabatic with entropy per baryon s in units of Boltzmann's constant and velocity as a function of distance from the black hole r to be $v = v_\infty(1 - r_0/r)^\beta$, where r_0 is the starting position on the disk, v_∞ is the final coasting velocity of $0.1c$, and β determines the outflow acceleration. Lower β corresponds to a more rapidly accelerating outflow while higher β is more slowly accelerating. This parameterization is qualitatively similar to numerical outflows models such as those in Barzilay & Levinson (2008). Fig. 3 shows a sample trajectory for outflow from the neutrino surface. We expect the direction of the outflow to be vertical close to the disk and radially outward far from it. Therefore in constructing our trajectories we take the outflow to be vertical initially, switching over to radial at a distance of twice the density scale height above the disk (though we note the resulting nucleosynthesis is not particularly sensitive to the choice of turnover point). As can be seen from this figure, the electron fraction is set by the weak rates relatively close to the surfaces, but nucleosynthesis takes place considerably further out. The dominant effect of the weak rates is from neutrino and antineutrino capture. The neutrino fluxes necessary to calculate these rates are determined by integrating over the contribution from the neutrinos emitted from all points on the neutrino surfaces. We calculate the element synthesis using a nuclear statistical equilibrium code, a charged particle reaction code, and finally an r-process network code as described in Surman et al. (2006). Given the asymmetry apparent in Figs. 1 and 2, it is clear that the trajectories from different starting points will produce different nucleosynthesis results. Therefore, for a given starting radius r_0, we run the complete calculation eight times, for starting points at eight different equally spaced angles around the disk. We then take the eight different nucleosynthesis outcomes and average them. In doing so we assume that material is not ejected preferentially on one particular side of the disk. When hydrodynamic calculations of winds from these disks become available, this averaging will no longer be necessary.

4. Results and Discussion

We have undertaken a wide survey of the nucleosynthesis from a variety of trajectories with conditions $0.2 \le \beta \le 1.4$, $10 \le s \le 50$, and 20 km $\le r_0 \le$ 80 km. In choosing these ranges we are guided by the results of Pruet et al. (2004); Metzger et al. (2007); Barzilay & Levinson (2008) for neutrino- and pressure-driven flows. We have found our results can be divided into two categories: those that produce a weak r-process and those that produce a main r-process. Examples of each type are shown in Fig. 4. While in this figure we have taken the average of the results for trajectories with eight different starting points, we find r-process nuclei produced in all trajectories.

The Y_e in the outflow is determined by the balance of the weak interactions. In this case ν_e and $\bar{\nu}_e$ capture eventually dominates over e^+ and e^- capture because the former have higher temperatures in the region above the torus. The neutrino capture rates for the relevant energy scales are approximately $\propto n_\nu T_\nu^2$; for more detail see McLaughlin et al. (1996). In the present merger scenario, not only is $T_{\bar{\nu}_e}$ substantially greater than T_{ν_e}, but $n_{\bar{\nu}} > n_\nu$ as well. Therefore in all cases $\bar{\nu}_e + p \rightarrow n + e^+$ is faster than $\nu_e + n \rightarrow p + e^-$ above the disk and the outflow becomes neutron rich (McLaughlin & Surman 2005; Setiawan et al. 2006). If these conditions were not met, the outflow could have become proton rich, as can happen in other astrophysical environments (Fröhlich et al. 2006; Buras et al. 2006). The electron fractions for a number of our trajectories at the point of nuclear recombination ($Y_{e,nr}$) and at the onset of the r-process ($Y_{e,f}$) are given in Table 1.

Weak r-process nuclei are produced in low entropy or fast acceleration conditions, and a main r-process is produced in between these two extremes. In all cases we take the initial electron fraction to be that given by the numerical model for the accretion torus. However, the weak interactions are sufficiently rapid that the electron fraction becomes reset in the outflow. When material first leaves the torus, the electron fraction spikes due to electron and positron capture, then later as the neutrinos dominate, Y_e falls. Both outflow timescale (i.e. β) and entropy have an impact on the electron fraction. The primary effect of outflow timescale is to influence the number of neutrino interactions that the nucleons can have. In the case of fast acceleration, there is relatively little time for neutrino capture on nucleons, so Y_e does not fall as far, and only a weak r-process is produced. For the conditions considered here, the entropy has two effects: it determines the initial spike in the electron fraction and it influences the point at which nuclei start to form. In the case of low entropy, nuclei form early and so the alpha effect, see e.g. McLaughlin et al. (1996), which drives up the electron fraction, is strong. This prevents the production of a full r-process. We note that while decreasing the timescale will weaken the alpha effect by allowing fewer neutrino captures during the epoch of alpha particle formation, it also decreases the number of neutrino captures before alpha particle formation. This means that the electron fraction never becomes sufficiently low to create a main r-process. Thus it is only for high entropy

Table 1. Electron fractions for a sample of trajectories with $r_0 = 40$ km.

S	β	$Y_{e,nr}$	$Y_{e,f}$
10	0.8	0.14 - 0.19	0.32 - 0.36
10	1.4	0.14 - 0.19	0.39 - 0.42
40	0.8	0.23 - 0.29	0.27 - 0.31
40	1.4	0.17 - 0.19	0.23 - 0.26

($s \geq 30$) and moderately accelerating trajectories ($\beta \geq 0.8$) that a main r-process occurs.

5. Conclusions

We find that for BH-NS mergers, almost all possible wind trajectories from the inner regions of the disk result in at least a weak r-process. This result is directly attributable to the neutrino physics. Should the connection between short duration GRBs and BH-NS mergers become firmly established, our results imply that short duration GRBs produce r-process elements.

In order for NS-NS mergers to be the sole contributor to the solar system weak r-process abundances, then $10^{-1}\,M_\odot$ to $1\,M_\odot$ must be ejected per merger, given a rate of 10^{-4} to 10^{-5} per year in the Galaxy (Belczynski et al. 2007). The rate of BH-NS mergers is less well constrained. However, given that current estimates of mass ejected from compact object mergers tend to be not more than $10^{-2}\,M_\odot$ (Ruffert et al. 1997; Oechslin et al. 2007), unless the rate is higher there is additional source of weak r-process material beyond BH-NS mergers. In any event the contribution of BH-NS mergers should be included in the Galactic tally of r-process abundances. Furthermore, if recent predictions for bimodal production processes for compact object mergers are confirmed (Belczynski et al. 2006), then there may be a contribution to the r-process early in the evolution of the Galaxy. This could influence the interpretation of the r-process pattern seen in halo star data.

Given that an r-process occurs in the hot outflows over such a wide range of our parameter study, a next step in determining the complete r-process abundance pattern produced by BH-NS mergers would be to add the calculations presented here together with estimates of the r-process from material ejected tidally during the merger. This requires future hydrodynamical simulations.

This work was partially supported by the Department of Energy under contracts DE-FG05-05ER41398 (RS) and DE-FG02-02ER41216 (GCM). This work was partially supported by the United States National Science Foundation under contract PHY-0244783 and AST-0653376 (WRH). Oak Ridge National Laboratory (WRH) is managed by UT-Battelle, LLC, for the U.S. Department of Energy under contract DE-AC05-000R22725.

REFERENCES

Argast, D., Samland, M., Thilemann, F.-K. & Qian, Y.-Z. 2004, A&A, 416, 997

Artemova, I.V., Björnsson, G., & Novikov, I.D. 1996, ApJ, 461, 565

Barzilay, Y. & Levinson, A. 2008, New A, in press (arXiv:0708.2996)

Belczynski, K., O'Shaughnessy, R., Kalogera, V., Rasio, F., Taam, R., & Bulik, T. 2007, Science, submitted (arXiv:0712.1036)

Belczynski, K., Perna, R., Bulik, T., Kalogera, V., Ivanova, N., & Lamb, D. 2006, ApJ, 648, 1110

Buras, R., Janka, H.-T., Rampp, M., & Kifonidis, K. 2006, A&A, 457, 281

Fröhlich, C., Martínez-Pinedo, G., Liebendörfer, M., Thielemann, F.-K., Bravo, E., Hix, W. R., Langanke, K., & Zinner, N. T. 2006, Phys. Rev. Lett., 96, 142502

Freiburghaus, C., Rosswog, S., & Thielemann, F.-K. 1999, ApJ, 525, L121

Goriely, S., Demetriou, P., Janka, H.-Th., Pearson, J.M., & Samyn, M. 2005, Nucl. Phys. A, 785, 587

Janka, H.-Th., Eberl, Th., Ruffert, M. & Fryer, C. L. 1999, ApJ, 527, 39

Lattimer, J. M. & Schramm D. N. 1974, ApJ, 192, L145

Lattimer, J. M. & Schramm D. N. 1976, ApJ, 210, 549

McLaughlin, G. C., Fuller, G. M., & Wilson, J. R. 1996, ApJ, 472, 440

McLaughlin, G. C. & Surman, R. 2005, Nucl. Phys. A, 758, 189

Meyer, B. S. 1989, ApJ, 343, 254

Metzger, B. D., Thompson, T. A., & Quataert, E. 2007, ApJ, 659, 561

Nakar, E. 2007, Phys. Rep., 442, 166

Oechslin, R., Janka, H.-Th., & Marek, A. 2007, A&A, 467, 395

Pruet, J., Thompson, T. A., & Hoffman, R. D2̇004, ApJ, 606, 1006

Qian, Y.-Z. & Wasserburg, G. J. 2007, Phys. Rep., 442, 237

Rosswog, S., Freiburghaus, C., & Thielemann, F.-K. 2001, Nucl. Phys. A, 688, 344

Ruffert, M., Janka, H.-Th., & Schäfer, G. 1996, A&A, 311, 532

Ruffert, M., Janka, H.-Th., Takahashi, K., & Schafer, G. 1997, A&A, 319, 122

Ruffert, M. & Janka, H.-Th. 2001, A&A, 380, 544

Setiawan, S., Ruffert, M., & Janka, H.-Th. 2006, A&A, 458, 553

Shen, H., Toki, H., Oyamatsu, K., & Sumiyoshi, K. 1998, Nucl. Phys. A, 637, 435

Surman, R. & McLaughlin, G. C. 2005, ApJ, 618, 397

Surman, R. & McLaughlin, G. C. 2004, ApJ, 603, 611

Surman, R., McLaughlin, G. C. & Hix, W. R. 2006, ApJ, 643, 1057

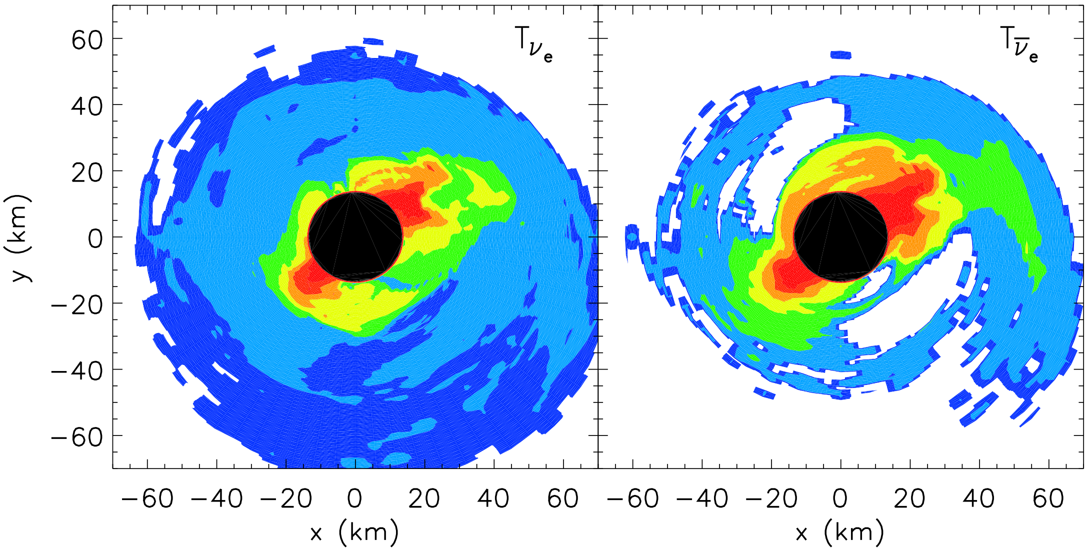

Fig. 1.— Plots of the electron neutrino (left panel) and electron antineutrino (right panel) temperature from the surface of the disk. Only regions where the neutrinos are trapped are shown. One can see from the figure that disks are asymmetric. Contours indicate regions, from darkest to lightest (or blue to red in color version), of temperatures of 1 MeV, 3 MeV, 5 MeV, 7 MeV, 9 MeV, 11 MeV and 13 MeV. The dark center indicates the inner boundary of the numerical merger model.

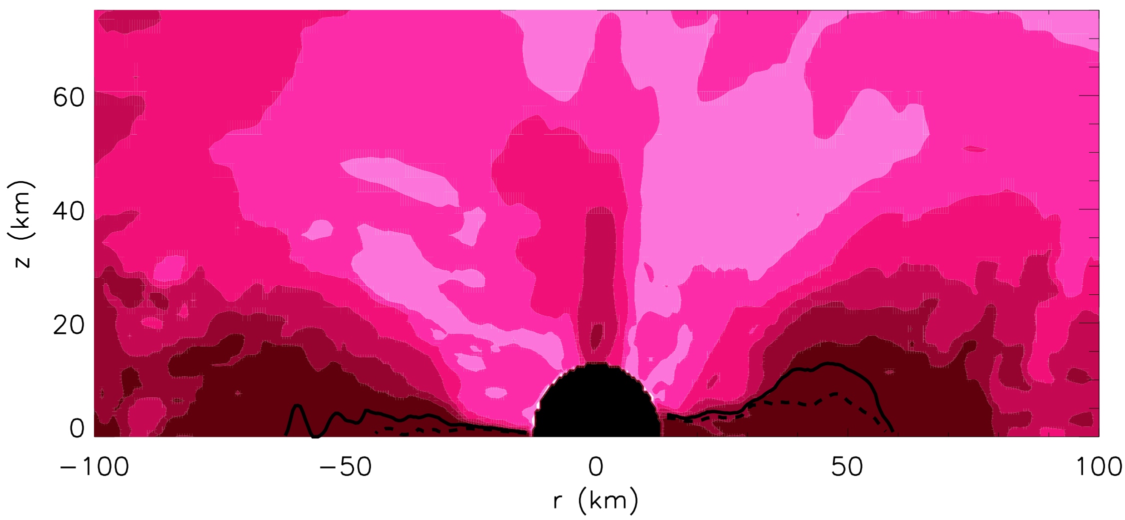

Fig. 2.— Shows density along a vertical slice of the disk. The shaded regions, from lightest to darkest, show densities of $10^{8.5}$, 10^{9}, $10^{9.5}$, 10^{10}, $10^{10.5}$, and 10^{11} g/cm^3. The solid line shows the electron neutrino surface while the dashed line shows the electron antineutrino surface. The dark center indicates the inner boundary of the numerical merger model.

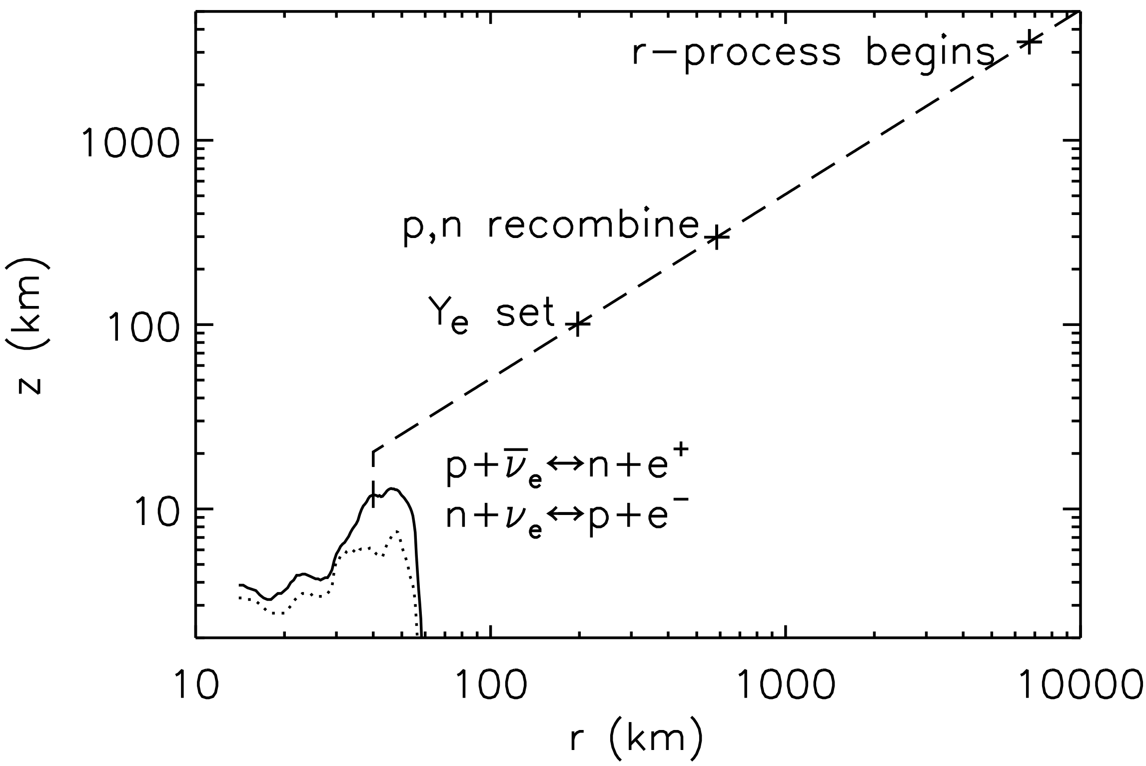

Fig. 3.— Shows a schematic representation of the neutrino and antineutrino surfaces, for the same vertical slice shown in Fig. 2 as well as an outflow trajectory, $\beta = 0.8$, $s = 20$. Indicated on the figure are the relative positions where the electron fraction is finished being set, where neutrons and protons recombine to begin to produce nuclei, and where the final stage of nucleosynthesis, the r-process, takes place.

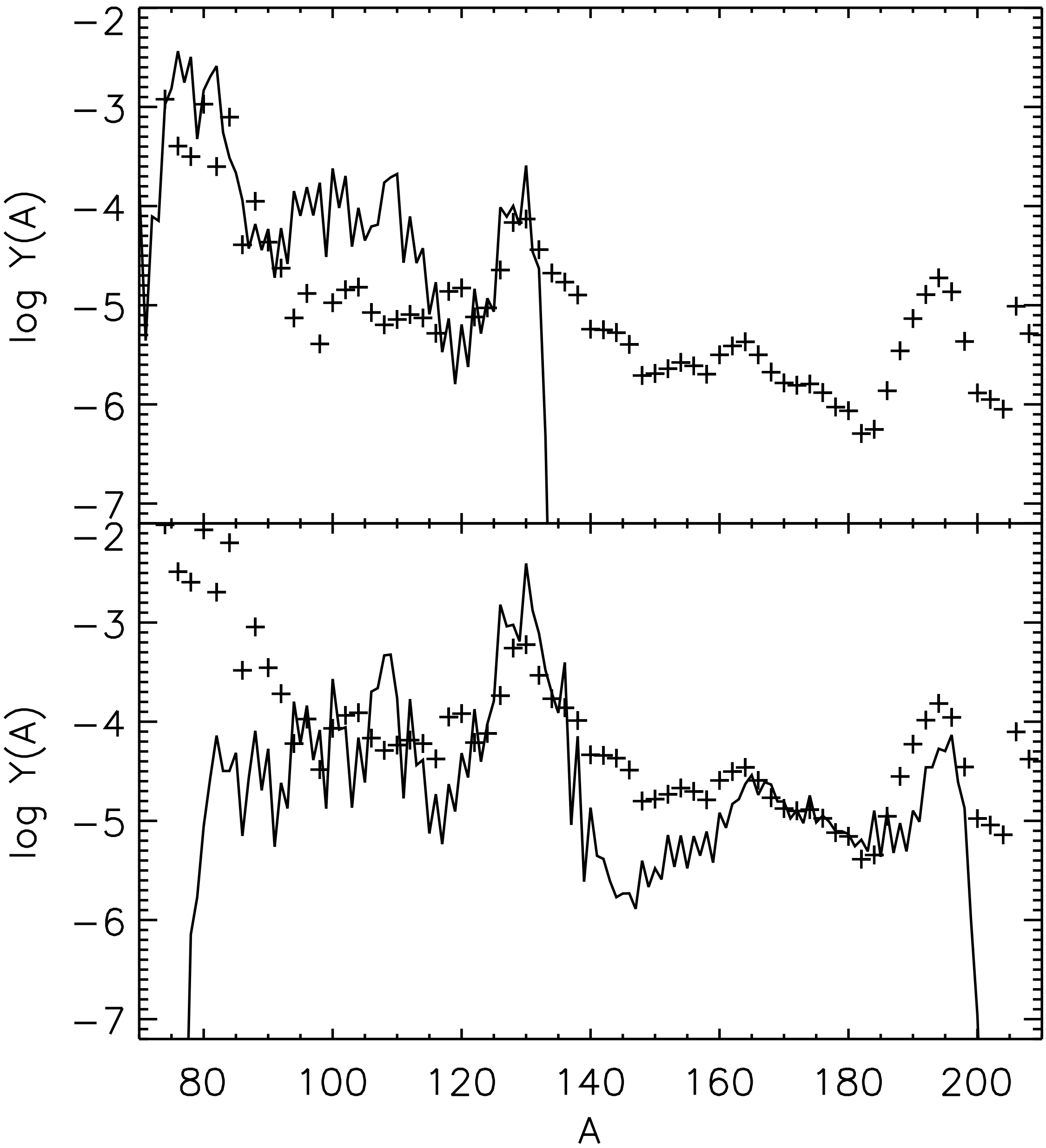

Fig. 4.— Plots of the nucleosynthesis calculation for outflow from the disk. The crosses represent the scaled solar system r-process abundances. The solid lines show the calculation. The top panel shows a weak r-process from conditions, $s = 20$, $\beta = 0.2$, angle averaged over the disk. This result is typical of outflow conditions where $s < 30$ or $\beta < 0.8$. The bottom panel shows a main r-process from the conditions, $s = 40$, $\beta = 0.8$, again angle averaged around the disk. This result is typical for conditions in the range $s = 30$ to $s = 50$, $\beta \geq 0.8$.